Hindawi
Journal of Food Processing and Preservation
Volume 2023, Article ID 5973846, 10 pages
https://doi.org/10.1155/2023/5973846

Research Article

Encapsulation of *Origanum compactum* Essential Oil in Beta-Cyclodextrin Metal Organic Frameworks: Characterization, Optimization, and Antioxidant Activity

Amine Ez-zoubi,[1] Saoussan Annemer,[1] Soukaina El Amrani,[2] Yassine Ez zoubi ,[1,3] and Abdellah Farah[1]

[1]*Laboratory of Applied Organic Chemistry, Faculty of Sciences and Techniques, Sidi Mohamed Ben Abdellah University, Route d'Imouzzer, Fez, Morocco*
[2]*Materials, Processes, Catalysis and Environment Laboratory, Higher School of Technology of Fez, Sidi Mohamed Ben Abdellah University, Imouzzer Road, 30000 Fez, Morocco*
[3]*Biotechnology, Environmental Technology and Valorization of Bio-Resources Team, Department of Biology, Faculty of Science and Techniques Al-Hoceima, Abdelmalek Essaadi University, Tetouan, Morocco*

Correspondence should be addressed to Yassine Ez zoubi; ezzoubiyassine@yahoo.fr

Received 1 October 2022; Revised 18 October 2022; Accepted 1 November 2022; Published 29 March 2023

Academic Editor: Charalampos Proestos

The study is aimed at enhancing the physicochemical and antioxidant properties of encapsulated *Origanum compactum* essential oil (OCEO). In this context, a Clevenger apparatus was operated in the hydrodistillation process for *O. compactum* extraction, and the aroma profile of essential oil was investigated using GC/MS and GC/FID. The encapsulation process was based on beta-cyclodextrin (βCD) and metal organic frameworks (K-βCD-MOFs), analyzed by several techniques. Furthermore, the response surface design allows for improved encapsulation efficiency by optimizing OCEO/K-βCD-MOFs (w/w) and water/ethanol ratios (v/v). The antioxidant activity of the essential oil, both before and after the encapsulation, was evaluated through 1,1-diphenyl-2-picrylhydrazyl. As a result, the highest EE ($35.34 \pm 1.23\%$) was achieved in 1/12 and 4/5 for OCEO/K-βCD-MOFs and water/ethanol, respectively. The increase in thermal stability also occurred along with the encapsulation of *O. compactum* essential oil. Compared with the free form, the *O. compactum* essential oil encapsulated in K-βCD-MOFs gradually showed higher antioxidant activity.

1. Introduction

Metal organic frameworks (MOFs) are crystalline coordination polymers with high porosity [1]. According to the combination of metal inorganic units and organic ligands, there are several areas in which MOFs can be applied: adsorption and separation [2], catalysis [3], molecular recognition [4], and drug delivery [5].

In order to minimize the risk of using organic ligands that have undesirable effects, [6] constructed MOFs based on cyclodextrins (CDs). In line with this, the CDs are cyclic oligosaccharides known as α-, β-, and γ-cyclodextrins, respectively, comprising six, seven, and eight α-1,4-connected D-glucopyranose units. Due to its cylindrical structure having a hydrophilic external surface and a hydrophobic core, the CDs are used to overcome the limitations of the essential oils which are the low aqueous solubility and chemical stability, as well as to facilitate their handling, moreover, to improve their biological properties and control release [7]. So, when CDs were in combination with a metal cation (K^+, Na^+, …, etc.), cyclodextrin organic metal framework CD-MOFs were generated.

Reports on the preparation of the encapsulation process through CD-MOFs have included various techniques such as impregnation, grinding, and cocrystallization methods [8]. During the molecular inclusion phase, factors

influencing the complexation reaction include preparation method, type of CD, alkali metals, temperature, and time of mixing. Therefore, the nature of alkali metals [9, 10] and the mass ratio [11, 12] were investigated during the encapsulation process through βCD-MOFs. In line with this, catechin (CA) has been encapsulated in α-, β-, and γ-CD-MOFs, while the highest encapsulation efficiency is displayed by K-βCD-MOFs [13]. In addition, K-βCD-MOFs were investigated as a promising delivery system for aroma compounds by studying the menthol release, and it is found that menthol/K-βCD-MOFs had a higher release control than menthol/βCD and pure menthol [11]. Furthermore, the lavender essential oil (LEO) was microencapsulated by K-βCD-MOFs to enhance the stability and antioxidant activity of LEO [14].

The genus Origanum belongs to the family Lamiaceae, described by five species, three of them are endemic to Morocco, including *Origanum compactum* commonly known as "Zaatar" [15]. *Origanum compactum* essential oil (OCEO) exhibited the existence of several phenolic compounds such as thymol and carvacrol and showed biological effects and antibacterial, antifungal, insecticidal, and antioxidant properties [16, 17]. The excellent biological activity makes *Origanum compactum* essential oil (OCEO) a promising candidate for the food industry. However, applications of OCEO are severely limited because of its high volatility and low water solubility. Consequently, encapsulation is needed to enhance its physicochemical and preserve biological properties. For food acceptability and nontoxicity, a novel class of β-CD-based biofriendly relevant metal organic frameworks (MOFs) composed has emerged as a new type of highly versatile material with large specific surface area and easily adjustable porous structures. According to literature [18], βCD-MOFs have several benefits, such as high inclusion and loading abilities. In addition, they are environmentally safe based on food-grade materials without producing toxic reagent residue.

Inspired by the previous studies, OCEO was encapsulated within βCD and K-βCD-MOFs by coprecipitation and impregnation methods, respectively. Additionally, the response surface design was used to achieve high encapsulation efficiency by optimizing the ratio among OCEO/K-βCD-MOFs and water/ethanol. Furthermore, the antioxidant activity of OCEO encapsulation process was assessed by DPPH revealing the practical improvement in the biological accessibility of OCEO.

2. Material and Methods

2.1. Chemicals Used. β-Cyclodextrin (βCD, min. 98%) was purchased from APPLICHEM. Potassium hydroxide (KOH, min. 85%), dichloromethane (CH_2Cl_2, min. 99.8%), and 1,1-diphenyl-2-picrylhydrazyl (DPPH, min. 90%) were provided by Sigma-Aldrich.

2.2. Extraction of O. compactum EO and Identification by GC-MS. Plant material of the *O. compactum* was collected in the commune of Timezgana (Taounate, Morocco) and was submitted to hydrodistillation for 3 hours, employing a modified Clevenger type apparatus. The *O. compactum* EO recovered was dehydrated using anhydrous sodium sulfate. The resulting essential oil was opacified in small vials and stored at 4°C under the name OCEO.

Gas chromatography coupled to mass spectrometry (GC-MS) was performed to identify the chemical composition of OCEO, under the same conditions described previously [19].

2.3. Synthesis. The synthesis of K-βCD-MOFs, its activation, and the encapsulation process of OCEO by βCD and K-CD-MOFs were presented in this section.

K-βCD-MOFs were prepared as mentioned by [20]; βCD and KOH (1 : 8 in molar ratio) were dissolved in deionized water (50 mL) and stirred gently for 2 h. Then, the obtained solution was filtered through a syringe filter membrane, followed by methanol vapor diffusion in a glass jar. Second, the colorless crystals are immersed in dichloromethane for 2 days and promoted using a 3-fold methanol wash of the K-βCD-MOF crystals (Figure 1).

The OCEO was encapsulated in K-βCD-MOFs by impregnation method as described by [21] with minor modifications. Briefly, OCEO (1 μL/mg) and K-βCD-MOFs were based on a range of mass ratios and were sonicated for 10 min in 5 mL (water/ethanol). Then, the mixture was treated gently (100 rpm) at 30°C in an incubator for 12 h. Finally, the obtained inclusion complexes are precipitated followed by filtration and dehydration at 50°C. On the other hand, the encapsulation procedure of OCEO by βCD (OCEO/βCD) was defined as follows: the OCEO was added dropwise to the aqueous solution of βCD (0.76 g of βCD in 20 mL of distilled water).

2.4. Encapsulation Efficiency. Encapsulated OCEO molecules in βCD and K-βCD-MOFs were examined as described by [22]; 10 mg of ICs was dissolved in anhydrous ethanol (100 mL) and sonicated for 30 min at 50°C. The obtained solution was centrifuged and filtered out the insoluble part of the sample. The amount of OCEO (m) molecules present in the ethanolic solution was quantified by the measurement of the absorbance with a spectrophotometer at $\lambda_{max} = 444$ nm.

Equation (1) was calculated to determine the encapsulation efficiency (EE).

$$\mathrm{EE}\,(\%) = \frac{m}{m_{\mathrm{OCEO}}} \times 100. \quad (1)$$

2.5. Characterization of K-βCD-MOFs and the ICs. To ensure the establishment of K-βCD-MOFs, as well as the inclusion procedure of OCEO via βCD and K-βCD-MOFs, the morphological examination of wall materials (βCD and K-βCD-MOFs), also their inclusion products OCEO/βCD and OCEO/K-CD-MOFs, was carried out by scanning electron microscope SEM (JSM-IT500HR) combined with an energy dispersive spectrometer (EDX). The samples were placed under a high vacuum at acceleration voltage 16 kV and a magnitude of 1000x. The Fourier transform infrared spectroscopy spectra FTIR (VERTEX 70–BRUKER) of the

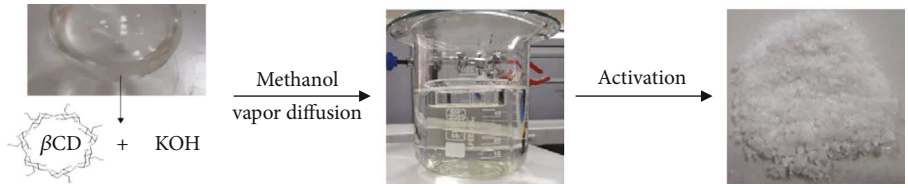

Figure 1: The three stages of K-βCD-MOF synthesis.

samples above and OCEO were processed by the KBr-pellet method, at a resolution of 4 cm^{-1}, and 32 scans were achieved from 400 to 4000 cm^{-1}. Thermogravimetric analysis (TGA) of samples was performed by LINSEIS STA PT1600 in an air atmosphere and heated at a rate of 10°C per minute from 20 to 700°C.

2.6. Determination of Antioxidant Activity Using DPPH Method. The antioxidant capacity of OCEO, OCEO/βCD, and OCEO/K-βCD-MOFs was carried out using the synthetic free radical synthetic 1,1-diphenyl-2-picrylhydrazyl (DPPH) according to the method reported by [23]. This method was employed to test EO's ability to scavenge free radicals, by the reduction of a DPPH methanolic solution in the presence of molecules that donate hydrogen. Briefly, each sample of essential oil was serially prepared in methanol (v/v) and mixed with 2 mL of DPPH (0.004%). The optical density at 517 nm was further determined using a UV spectrophotometer after allowing the mixtures to remain at room temperature in the dark for 30 minutes. All samples were tested in three replicates for each concentration. The inhibitory concentration 50 (IC_{50}) value represents the dose of EO that neutralizes 50% of DPPH radicals. The IC_{50} was used as an estimate of the antioxidant activity per DPPH and was estimated by extrapolation of the percent inhibition (I%) versus concentrations (C). The percentage of DPPH free radical inhibition (I%) was calculated as follows [24]:

$$I(\%) = \frac{\text{Ac} - \text{As}}{\text{Ac}} \times 100, \quad (2)$$

where Ac and As were the absorbance of DPPH (as control) and absorbance of the sample, respectively.

2.7. Response Surface Design Study. In this part, based on the mass ratio of OCEO to K-βCD-MOFs, as well as the volume ratio of ethanol and water, we have been charged to improve the encapsulation efficiency of OCEO through K-βCD-MOFs. Thus, all of the experimental data from the response surface design of type central composite design was evaluated using Design Expert version 13 software. The two factors studied, also the low, high, and center levels of the factors, are shown in Table 1.

Composite designs therefore have three parts (Table 2); the factorial design has two levels per factor and can be either complete or fractional. The points in the center of the study domain and the points of the star design are on the axes, placed at the same distance from the center of the study domain.

Table 1: Experimental levels of independent parameters.

Factor	Level -1	Level 0	Level +1
Factor 1: water/ethanol	1/5	1/2	4/5
Factor 2: OCEO/K-βCD-MOFs	1/1	1/6.5	1/12

Table 2: Centered composite design for two factors.

N° EXP	Factor 1	Factor 2
1	-1	-1
2	+1	-1
3	-1	+1
4	+1	+1
5	0	0
6	0	0
7	-1.21	0
8	+1.21	0
9	0	-1.21
10	0	+1.21
11	0	0
12	0	0

The postulated mathematical model is a second-degree model:

$$Y = a_0 + \sum_{i=1}^{2} a_i x_i + \sum_{i=1}^{2} a_{ij} x_i x_j + \sum_{i=1}^{2} a_{ii} {x_i}^2 + \varepsilon. \quad (3)$$

The selected response is the encapsulation efficiencyEE% represented by Y,a_0,a_i,a_{ij}, and a_{ii}, representing the regression coefficients for the constant term, interaction effects, and second-order effects, respectively.x_1 and x_2 are the coded independent parameters studied, and ε is an error term. The fitted model was evaluated using an analysis of variance (ANOVA). The F value is used to determine whether the model is highly significant and whether the parameters adequately explain the variation of the data from their mean. The quality of the fitted model and its prediction were assessed by the coefficients of determination (R^2 and adjusted R^2) [25].

2.8. Statistical Analysis. All of the experimental data were evaluated statistically through analysis of variance (ANOVA) using SPSS software. All the values were presented as average value ± standard deviation (SD), with $p \leq 0.05$% considered statistically significant.

Table 3: Chemical composition of OCEO investigated by GC-MS.

Compounds	Retention index	Percentage (%)
α-Thujene	926	0.08
α-Pinene	939	2.39
Camphene	953	0.23
1-Octene-3-ol	978	0.11
β-Pinene	980	0.23
β-Myrcene	991	0.92
α-Phellandrene	1005	0.16
δ-3-Carene	1010	0.13
α-Terpinene	1018	3.45
p-Cymene	1026	12.01
Limonene	1031	0.23
1,8-Cineole	1033	0.05
γ-Terpinene	1062	18.86
Terpinolene	1088	0.21
Linalol	1098	0.26
Camphre	1136	0.17
Borneol	1165	0.40
Terpinen-4-ol	1177	0.30
α-Terpineol	1189	0.23
Thymol	1290	29.56
Carvacrol	1298	26.44
β-Caryophyllene	1418	1.95
γ-Cadinene	1513	0.12
Caryophyllene oxide	1581	0.11

3. Results and Discussion

3.1. Aroma Profile of O. compactum Essential Oil. The chemical composition of OCEO was revealed twenty-four components representing 98.60% of the total oil. As shown in Table 3, each compound was characterized by its retention index and percentage; thymol, carvacrol, γ-terpinene, and p-cymene are the four major compounds found in OCEO with 29.56, 26.44, 18.86, and 12.01%, respectively. The results of the analysis are similar to those reported in the previous studies [17, 26].

3.2. Characterization of K-βCD-MOFs and Inclusion Complex

3.2.1. Scanning Electron Microscopy. The Scanning electron microscopy method could be very useful to confirm morphological differences caused by interactions between components [27]. The SEM photographs of βCD, K-βCD-MOFs, OCEO/βCD, and OCEO/K-βCD-MOFs as shown in Figure 2 indicated that the inclusion complex of OCEO affects the guest morphology, by the establishment of clusters out of shape and reduction of sizes.

Furthermore, the energy dispersive X-ray (EDX) verified the process of crosslinking potassium to βCD as illustrated in Figure 3. The mass and atomic percentages of potassium K were $1.37 \pm 0.10\%$ and $0.49 \pm 0.04\%$, respectively.

3.2.2. Fourier Transform Infrared Spectroscopy. The Fourier transform infrared spectroscopy was employed to evaluate the formation of the inclusion complex of OCEO in βCD and K-βCD-MOFs. So, the infrared spectra of K-βCD-MOFs (Figure 4) were characterized by a broad absorption peak at 3280 cm^{-1} belonging to O-H stretching vibration, other peak at 2925 and 1649 cm^{-1} accounting for C-H and H-O-H stretching vibrations. The same absorption bands were shown in βCD spectra with minor modifications in position. This is attributed to the fact that K-βCD-MOF synthesis retained the core skeleton of βCD. The infrared absorption of OCEO was exhibited at 3320 cm^{-1} stretching vibrations of O-H phenolic group, also at 3020 and 2958 cm^{-1} corresponding to =C-H and C-H stretching bands, respectively. As previously indicated, OCEO is mainly composed of thymol and carvacrol. During the formation of inclusion complex (OCEO/βCD, OCEO/K-βCD-MOFs), the absorption bands of the host (βCD and K-βCD-MOFs) were changed either in position, intensity, and shape; also, the C-H stretching band was altered as shown in Figure 4. Similar studies [12, 28] were indeed the procedure for inclusion of OCEO within βCD and K-βCD-MOFs.

3.2.3. Thermal Analysis. The thermogravimetric analysis (TGA) was used to evaluate the thermal stability of OCEO before and after the encapsulation process. Figure 5 shows that the major fraction of OCEO (78.8%) was evaporated up to 176°C. From the TG spectra for βCD, a first mass loss (14%) associated with the release of water (115°C) can be observed. The thermal decomposition of βCD was detected after 287°C, when 78% were lost from initial mass. Besides, the thermogram of K-βCD-MOFs showed the first mass loss until 108°C corresponds to the expulsion of methanol and water. The second weight loss above 218°C was combined with the organic component of the K-βCD-MOFs. The remaining material that slowly decreased after this second drop was the inorganic potassium, which needed higher temperatures to completely degrade. On the other hand, compared with OCEO/βCD and OCEO/K-βCD-MOFs, the thermal stability of OCEO was improved during the inclusion process, and the thermal evaporation of OCEO is shifted to a considerably higher temperature (~280°C). The analysis of thermogravimetric (TG) curves supports the successful entrapment of OCEO into βCD and K-βCD-MOFs.

3.3. Statistical Validation. The results of the experiments are presented in Table 4. The tests have been shown in the classical order of the centered composite design.

The main effect of the regression is significant, according to the finding in the analysis of variance (Table 5), as the probability of risk significance p value is less than 0.05. In addition, the lack of fit of the postulated models was 1.23, corresponding to probabilities of 0.44 (Table 5). This signifies that the lack of fit of the adopted models was not significant. The coefficient of determination $R^2 = 98.69\%$ is sufficient, and this value provides good compatibility between the experimental results and predicted values of the fitted model.

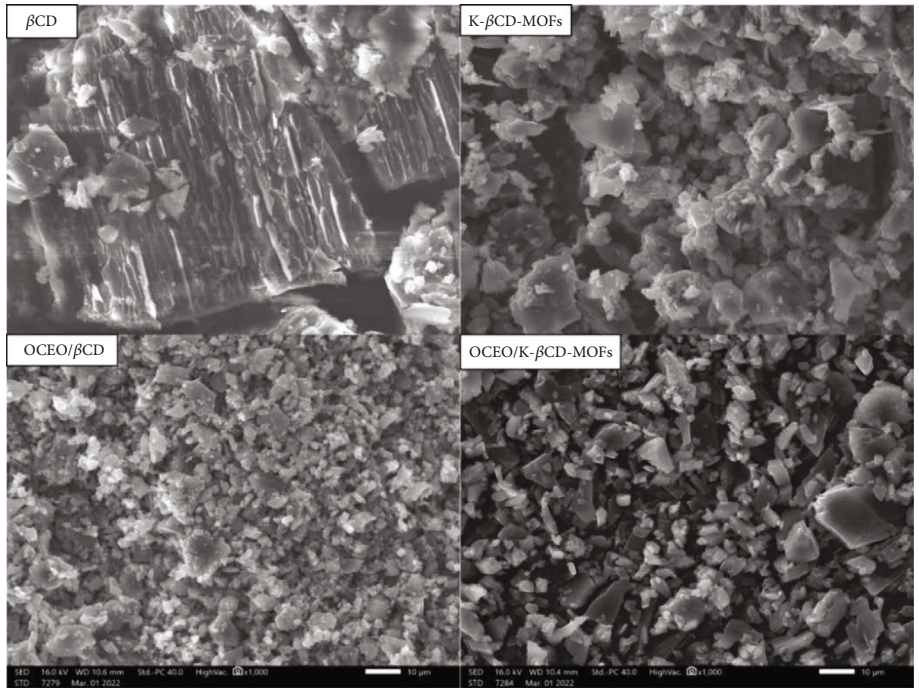

Figure 2: SEM micrographs of βCD, K-βCD-MOFs, OCEO/βCD, and OCEO/K-βCD-MOFs.

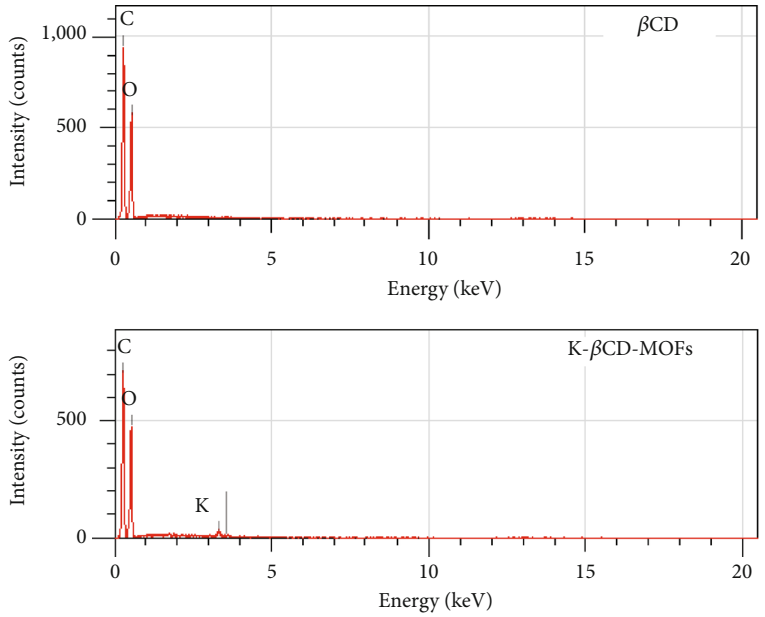

Figure 3: EDX spectra of βCD and K-βCD-MOFs.

The graph (Figure 6) confirms that the curve of the observed values related to predicted values has the perfect appearance of a straight line.

Table 6 gives a summary of the effects of all factors investigated as well as the statistical values of the *t*-student and the observed probability (*p* value). According to this table, all coefficients in the model are statistically significant (*p* value < 0.05), so all coefficients were intended to be present in the postulated model.

Thus, the mathematical model retained was presented by the following equation:

$$EE\% = 26.21 + 0.82x_1\ 4.24\,x_2 + 1.83\,x_1x_2 + 3.75\,x_1^{\ 2} - 1.28\,x_2^{\ 2}. \tag{4}$$

The objective of this part is to find the optimal adjustment of the two parameters that allows a high encapsulation

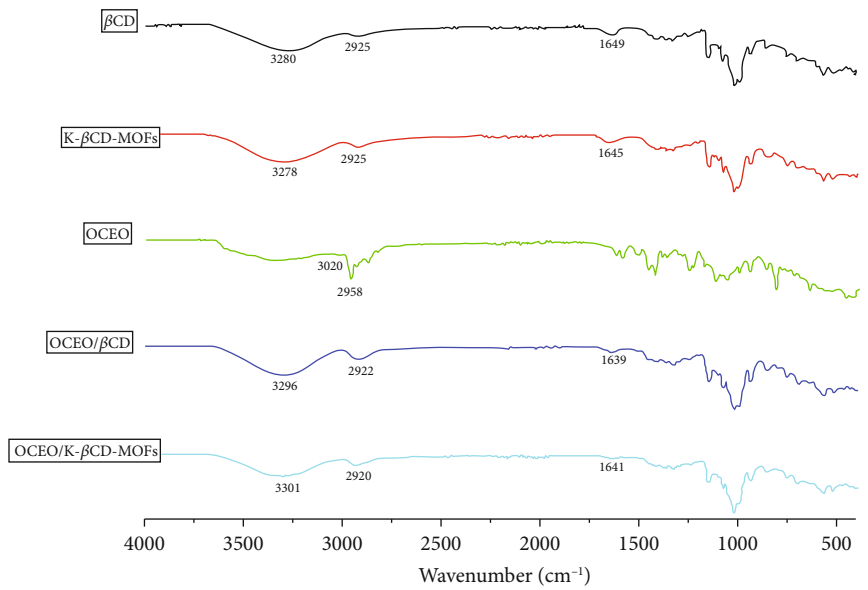

Figure 4: FTIR spectra of βCD, K-βCD-MOFs, OCEO, OCEO/βCD, and OCEO/K-βCD-MOFs.

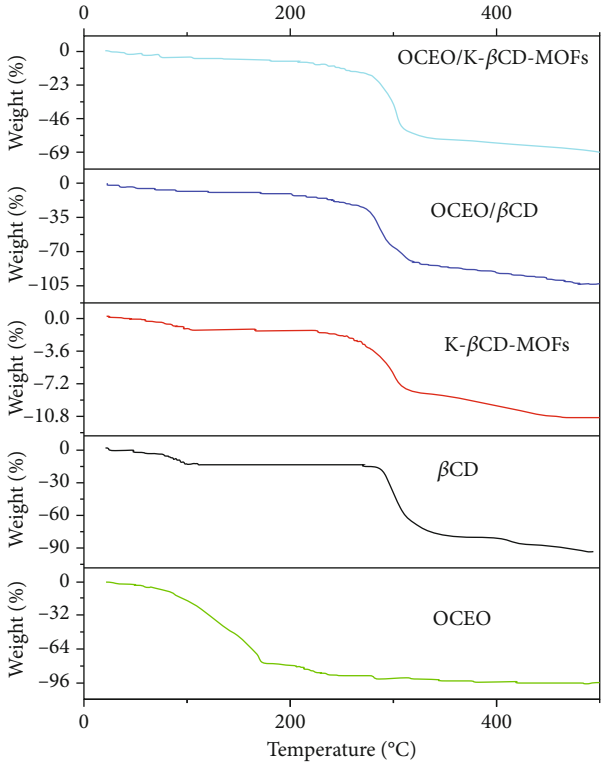

Figure 5: TGA thermogram of OCEO βCD, K-βCD-MOFs, OCEO/βCD, and OCEO/K-βCD-MOFs.

efficiency. By using the cube and 3D graphs (Figure 7), we can also explore other conditions.

Figure 7 illustrates that obtaining the desired efficiency requires maximization of the water/ethanol and OCEO/K-CD-MOF ratios. The area of the desired compromise for the two parameters exists in the area of the cube formed by the area where the water/ethanol and OCEO/K-CD-MOF ratios are maximal.

Table 4: Experimental results and experience matrix.

N° EXP	Water/ethanol	OCEO/K-βCD-MOFs	Encapsulation efficiency (%)
1	1/5	1/1	24.96 ± 1.21
2	4/5	1/1	23.00 ± 2.01
3	1/5	1/12	30.00 ± 4.31
4	4/5	1/12	35.34 ± 1.23
5	1/2	1/6.5	26.52 ± 2.63
6	1/2	1/6.5	26.32 ± 2.12
7	1.21/5	1/6.5	31.21 ± 3.46
8	4.84/5	1/6.5	33.12 ± 2.20
9	1/2	1/1.21	19.83 ± 1.44
10	1/2	1/14.52	29.77 ± 1.26
11	1/2	1/6.5	26.36 ± 2.89
12	1/2	1/6.5	25.12 ± 1.76

Table 5: Analysis of variance for the postulated model.

Source	Degrees of freedom	Sum of square	Mean square	F ratio	p value
Model	5	210.08	42.02	90.51	<0.0001
Error	6	2.79	0.46		
Total	11	212.86			
Lack of fit	3	0.51	3,23	1.23	0.44
Pure error	3	1.25	0.42		
R^2	98.69%				
R_{adj}^2	97.60%				
Standard deviation	0.68				

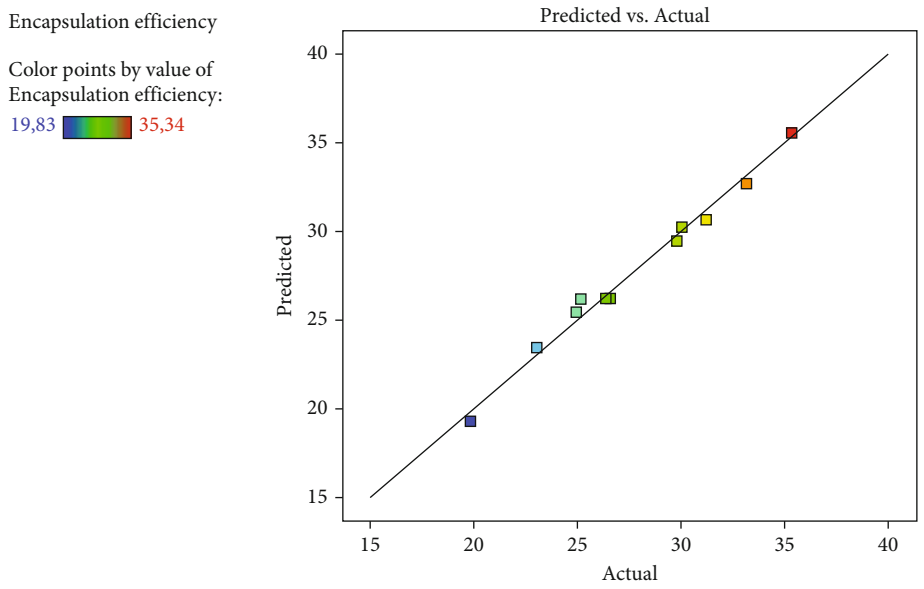

Figure 6: Observed vs. predicted values for encapsulation efficiency.

Table 6: Effects of model coefficients linking response to factors.

Term	Coefficient	Estimation	Error standard	t-student	p value
Constant	a_0	26.21	0.33	72.31	<0.0001
X_1: water/ethanol	a_1	0.82	0.26	2.94	0.0259
X_2: OCEO/K-βCD-MOFs	a_2	4.24	0.26	15.20	<0.0001
Water/ethanol* OCEO/K-βCD-MOFs	a_{12}	1.83	0.34	4.97	0.0025
Water/ethanol*water/ethanol	a_{11}	3.75	0.33	10.94	<0.0001
OCEO/K-βCD-MOFs * OCEO/K-βCD-MOFs	a_{22}	-1.28	0.33	-3.24	0.0178

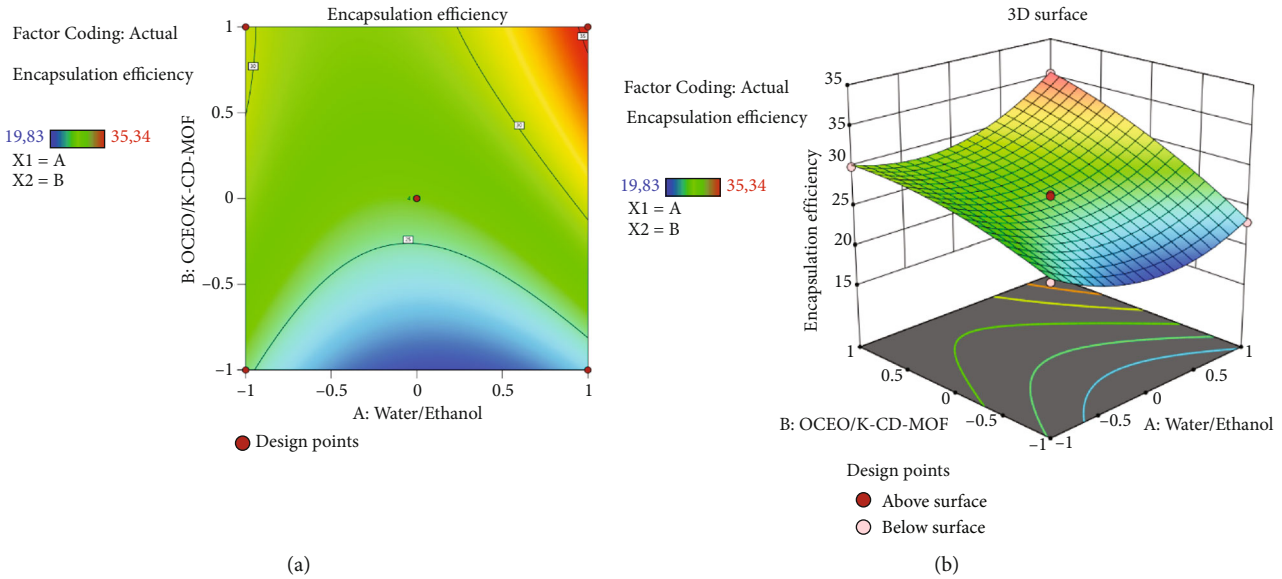

Figure 7: 2D and 3D representations of the optimized parameters leading to the desired encapsulation efficiency.

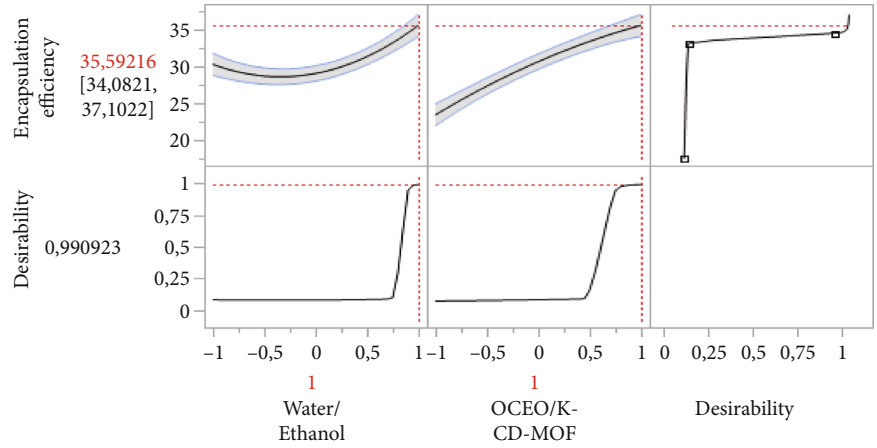

Figure 8: Profile for predicting optimal conditions for encapsulation efficiency.

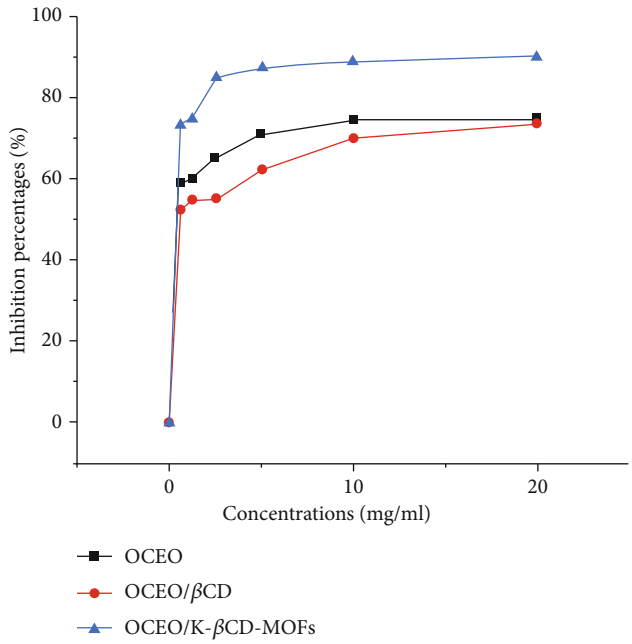

Figure 9: The inhibition percentages of OCEO, OCEO/βCD, and OCEO/K-βCD-MOFs.

Figure 8 confirms that the achievement of this efficiency value is possible with a desirability of the order of 99% by ensuring the following setting:

(i) Water/ethanol ratio of 4/5

(ii) OCEO/K-CD-MOFs of 1/12

Thus, K-βCD-MOFs achieved a higher encapsulation efficiency ($35.34 \pm 1.23\%$) than βCD ($27.54 \pm 1.05\%$). As according the previous reports [29, 30], the encapsulation of active compounds through CD-MOFs is more efficient than CD alone.

3.4. DPPH Assay. In order to evaluate the radical scavenging potential of OCEO both in free and encapsulated forms, the reactivity towards the stable free radical DPPH was determined. The purple color of DPPH quickly fades in contact with proton radical; this scavenging action serves as the fundamental method for the assessment of antioxidant activity. The results of the DPPH radical inhibition from Figure 9 show that the percentage of inhibition increases with the concentration; it is a dose-dependent response, and all the three graphs have the same appearance.

Table 7: Inhibition concentration (IC_{50}) of OCEO, OCEO/βCD, and OCEO/K-βCD-MOFs.

Sample	IC_{50} (mg/mL)
OCEO	0.62
OCEO/βCD	0.54
OCEO/K-βCD-MOFs	0.44

The inhibitory concentration 50 values of the samples are shown in Table 7, and lower IC_{50} reflects a better level of antioxidant activity. As a result, OCEO/K-βCD-MOFs had the highest antioxidant potential with lower IC_{50} (0.44 mg/mL). For OCEO, the IC_{50} value was 0.54 mg/mL, and it was increased for OCEO/βCD (0.62 mg/mL).

This strong antioxidant effect of OCEO could be attributed mainly to the high percentages of phenolic components. Numerous research revealed a linear positive correlation between plant extract phenolic content and antioxidant strength [31]. Carvacrol and thymol the major compounds of OCEO are proved to act as strong antioxidants [32]. In brief, since essential oils are complex combinations of several types of chemicals, their antioxidant activity is typically the result of additive, synergistic, and/or antagonistic actions [15]. In contrast, the antioxidant activity of OCEO into βCD was reduced due to its incorporation within the cavity of cyclodextrin, which allows for limiting the reaction between the hydroxyls of these phenolic compounds including carvacrol and thymol with free radicals [33]. On the other hand, the K-βCD-MOFs enhance the antioxidant capacity of OCEO; this improvement could account for both that the K-βCD-MOFs did not interact with the hydroxyls groups of the essential oils, as well as the antioxidant nature of potassium. Consequently, further research into the use of

different metal nature should be done, in addition to the interactions between various phenolic compounds of OCEO and CDMOFs.

4. Conclusion

Metal organic frameworks based on βCD as a ligand combined with potassium (K) metal units have been prepared in this present study using methanol vapor diffusion approach. The OCEO was successfully encapsulated into βCD and K-βCD-MOFs, respectively, using coprecipitation and impregnation methods. Besides, the TGA results showed that both inclusion complexes exhibited higher thermal stability than OCEO. Compared to βCD, K-βCD-MOFs displayed higher encapsulation efficiency through optimizing the ratio of OCEO/K-βCD-MOFs (w/w) and ethanol/water (v/v) by response surface design. Furthermore, the antioxidant capacity of OCEO revealed by DPPH assay was significantly enhanced in the presence of K-βCD-MOFs. Therefore, the above results support the use of K-βCD-MOFs as a nontoxic biocompatible porous material in the food sector. Consequently, we will focus our future research to investigate the practicality and efficacy of OCEO encapsulated into K-βCD-MOFs for applications in food models.

Data Availability

The data used to support the findings of this study are available from the corresponding author upon request.

Additional Points

Novelty Impact Statement. The encapsulation of *Origanum compactum* essential oil into K-βCD-MOFs can enhance its loading capacity and antioxidant properties, compared with βCD. Consequently, an optimization study of the encapsulation process was performed to ensure the highest efficiency. Therefore, the antioxidant activity revealed by DPPH verified that OCEO/K-βCD-MOFs possess the most effective ability. The current research may advance the application of essential oil encapsulated by K-βCD-MOFs in the food industry.

Conflicts of Interest

The authors have no known competing financial interests.

Authors' Contributions

Ez-zoubi Amine wrote the original draft and was responsible for the formal analysis, investigation, conceptualization, and methodology. Saoussan Annemer was responsible for the validation and software. Soukaina El Amrani was responsible for the visualization and investigation. Yassine Ez zoubi was responsible for the validation and data curation and wrote, reviewed, and edited the manuscript. Abdellah Farah wrote, reviewed, and edited the manuscript and was responsible for the resources, conceptualization, and supervision.

References

[1] H. Musarurwa and N. T. Tavengwa, "Advances in the application of chitosan-based metal organic frameworks as adsorbents for environmental remediation," *Carbohydrate Polymers*, vol. 283, article 119153, 2022.

[2] Z. Zhang, S. B. Peh, C. Kang, K. Chai, and D. Zhao, "Metal-organic frameworks for C6-C8 hydrocarbon separations," *EnergyChem*, vol. 3, no. 4, article 100057, 2021.

[3] D. N. Dybtsev and K. P. Bryliakov, "Asymmetric catalysis using metal-organic frameworks," *Coordination Chemistry Reviews*, vol. 437, article 213845, 2021.

[4] N. Hosono and T. Uemura, "Metal-organic frameworks for macromolecular recognition and separation," *Matter*, vol. 3, no. 3, pp. 652–663, 2020.

[5] S. He, L. Wu, X. Li et al., "Metal-organic frameworks for advanced drug delivery," *Acta Pharmaceutica Sinica B*, vol. 11, no. 8, pp. 2362–2395, 2021.

[6] R. A. Smaldone, R. S. Forgan, H. Furukawa et al., "Metal–organic frameworks from edible natural products," *Angewandte Chemie, International Edition*, vol. 49, no. 46, pp. 8630–8634, 2010.

[7] M. Kfoury, L. Auezova, H. Greige-Gerges, and S. Fourmentin, "Encapsulation in cyclodextrins to widen the applications of essential oils," *Environmental Chemistry Letters*, vol. 17, no. 1, pp. 129–143, 2019.

[8] Y. Han, W. Liu, J. Huang et al., "Cyclodextrin-based metal-organic frameworks (CD-MOFs) in pharmaceutics and biomedicine," *Pharmaceutics*, vol. 10, no. 4, p. 271, 2018.

[9] W. Jiang, H. Liu, Q. Liao et al., "Preparation of two metal organic frameworks (K-β-CD-MOFs and Cs-β-CD-MOFs) and the adsorption research of myricetin," *Polyhedron*, vol. 196, article 114983, 2021.

[10] J.-Q. Sha, L.-H. Wu, S.-X. Li et al., "Synthesis and structure of new carbohydrate metal-organic frameworks and inclusion complexes," *Journal of Molecular Structure*, vol. 1101, pp. 14–20, 2015.

[11] Z. Hu, M. Shao, B. Zhang, X. Fu, and Q. Huang, "Enhanced stability and controlled release of menthol using a β-cyclodextrin metal-organic framework," *Food Chemistry*, vol. 374, article 131760, 2022.

[12] S. Wang, G. Shao, H. Zhao et al., "Covering soy polysaccharides gel on the surface of β-cyclodextrin-based metal–organic frameworks," *Journal of Materials Science*, vol. 56, no. 4, pp. 3049–3061, 2021.

[13] L. Jiang, F. Wang, M. Du et al., "Encapsulation of catechin into nano-cyclodextrin-metal-organic frameworks: preparation, characterization, and evaluation of storage stability and bioavailability," *Food Chemistry*, vol. 394, article 133553, 2022.

[14] Y. Wang, L. Wang, J. Tan, R. Li, Z.-T. Jiang, and S.-H. Tang, "Enhancement of the stabilities and intracellular antioxidant activities of lavender essential oil by metal-organic frameworks based on beta-cyclodextrin and potassium cation," *Polish Journal of Food and Nutrition Sciences*, vol. 71, 2021.

[15] F. E. Babili, J. Bouajila, J. P. Souchard et al., "Oregano: chemical analysis and evaluation of its antimalarial, antioxidant, and cytotoxic activities," *Journal of Food Science*, vol. 76, no. 3, pp. C512–C518, 2011.

[16] A. Bouyahya, G. Zengin, O. Belmehdi et al., "Origanum compactum Benth., from traditional use to biotechnological

applications," *Journal of Food Biochemistry*, vol. 44, no. 8, article e13251, 2020.

[17] S. El amrani, L. Sanae, Y. Ez zoubi et al., "Combined antibacterial effect of Origanum compactum and Mentha piperita (Lamiaceae) essential oils against ATCC Escherichia coli and Staphylococcus aureus," *Vegetos*, vol. 35, no. 1, pp. 74–82, 2022.

[18] Y. Wang, Y.-T. Du, W.-Y. Xue et al., "Enhanced preservation effects of clove (*Syzygium aromaticum*) essential oil on the processing of Chinese bacon (preserved meat products) by beta cyclodextrin metal organic frameworks (β-CD-MOFs)," *Meat Science*, vol. 195, article 108998, 2023.

[19] A. Ez-zoubi, Y. Ez zoubi, A. Ramzi, M. Fadil, A. E. O. Lalami, and A. Farah, "Ethanol and glycerol green emulsifying solvent for the formation of a *Lavandula stoechas* essential oil/ β-cyclodextrin inclusion complex: mixture design and adulticidal activity against *Culex pipiens*," *Heliyon*, vol. 8, no. 8, p. e10204, 2022.

[20] G. Shao, S. Wang, H. Zhao et al., "Tunable arrangement of hydrogel and cyclodextrin-based metal organic frameworks suitable for drug encapsulation and release," *Carbohydrate Polymers*, vol. 278, article 118915, 2022.

[21] N. Lv, T. Guo, B. Liu et al., "Improvement in thermal stability of sucralose by γ-cyclodextrin metal-organic frameworks," *Pharmaceutical Research*, vol. 34, pp. 269–278, 2017.

[22] H. Yin, C. Wang, J. Yue et al., "Optimization and characterization of 1,8-cineole/hydroxypropyl-β-cyclodextrin inclusion complex and study of its release kinetics," *Food Hydrocolloids*, vol. 110, article 106159, 2021.

[23] O. K. Taghzouti, M. Balouirib, W. Ouedrhiric, A. E. Chahadd, and A. Romanea, "In vitro evaluation of the antioxidant and antimicrobial effects of Globularia alypum L. extracts," *Journal of Materials and Environmental Science*, vol. 7, pp. 1988–1995, 2016.

[24] N. Ghazanfari, S. A. Mortazavi, F. T. Yazdi, and M. Mohammadi, "Microwave-assisted hydrodistillation extraction of essential oil from coriander seeds and evaluation of their composition, antioxidant and antimicrobial activity," *Heliyon*, vol. 6, no. 9, article e04893, 2020.

[25] S. S. Abu Amr, H. A. Aziz, and M. J. K. Bashir, "Application of response surface methodology (RSM) for optimization of semi-aerobic landfill leachate treatment using ozone," *Applied Water Science*, vol. 4, no. 3, pp. 231–239, 2014.

[26] J. Lazrak, E. H. El Assiri, N. Arrousse et al., "Origanum compactum essential oil as a green inhibitor for mild steel in 1 M hydrochloric acid solution: experimental and Monte Carlo simulation studies," *Materials Today: Proceedings*, vol. 45, pp. 7486–7493, 2021.

[27] A. Cid-Samamed, J. Rakmai, J. C. Mejuto, J. Simal-Gandara, and G. Astray, "Cyclodextrins inclusion complex: preparation methods, analytical techniques and food industry applications," *Food Chemistry*, vol. 384, article 132467, 2022.

[28] Y. Zhang, Q. OuYang, B. Duan et al., "*Trans*-2-hexenal/β-cyclodextrin effectively reduces green mold in citrus fruit," *Postharvest Biology and Technology*, vol. 187, article 111871, 2022.

[29] Y. Chen, K. Tai, P. Ma et al., "Novel γ-cyclodextrin-metal-organic frameworks for encapsulation of curcumin with improved loading capacity, physicochemical stability and controlled release properties," *Food Chemistry*, vol. 347, article 128978, 2021.

[30] Z. Hu, S. Li, S. Wang, B. Zhang, and Q. Huang, "Encapsulation of menthol into cyclodextrin metal-organic frameworks: preparation, structure characterization and evaluation of complexing capacity," *Food Chemistry*, vol. 338, article 127839, 2021.

[31] H. Sbayou, A. Boumaza, A. Hilali, and S. Amghar, "Antioxidant properties of Artemisia herba-alba Asso., Mentha pulegium L. and Origanum compactum Benth. essential oils," *Journal of Materials and Environmental Science*, vol. 7, pp. 2908–2912, 2016.

[32] M. G. Miguel, "Antioxidant and anti-inflammatory activities of essential oils: a short review," *Molecules*, vol. 15, no. 12, pp. 9252–9287, 2010.

[33] E. H. Santos, J. A. Kamimura, L. E. Hill, and C. L. Gomes, "Characterization of carvacrol beta-cyclodextrin inclusion complexes as delivery systems for antibacterial and antioxidant applications," *LWT - Food Science and Technology*, vol. 60, no. 1, pp. 583–592, 2015.